WIN 2002

21-26 January

Christchurch, New Zealand

V.Tumakov

University of California, Irnive

1. Motivation
2. Current experiments
3. The MECO experiment
4. Status and conclusion

Why Search for Lepton Flavor Violation ?

Experimental evidence shows there are nearly conserved additive quantum numbers associated with each *family* of leptons:

G=1	e	ν_e	u	d
G=2	μ	ν_μ	c	s
G=3	τ	ν_τ	t	b

- Rigorously true in the SM if neutrinos are mass degenerate.
- These conservation laws are empirical – no known gauge symmetry protects lepton flavor.
- Discovery of the neutrino oscillations stimulated the LFV search in charged lepton sector.
- LFV in extended Standard Model can occur through ν oscillation.

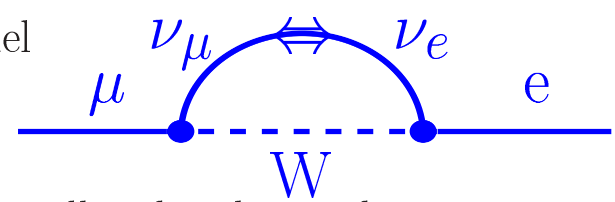

  – $\propto (m_\nu/m_W)^4 \approx 10^{-26}$ - too small to be observed

- Essentially all extensions to the SM allow LFV.

  – For example in SUSY-GUT:

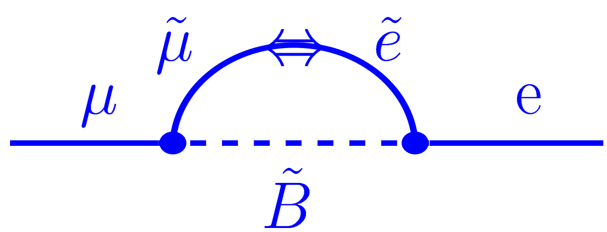

- Extensions to the Standard Model, including super-symmetric theories, that unify quarks and leptons lead to small but observable rates for μ-e conversion.

LFV Searched for in Many Processes

		M or ΔM Limit
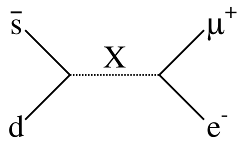	**BNL E871** $\mathbf{B(K^0_L \to \mu^\pm e^\mp) < 4.7 \times 10^{-12}}$	**150 TeV/c²**
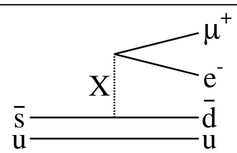	**BNL E865** $\mathbf{B(K^+ \to \pi^+ \mu^+ e^-) < 4.0 \times 10^{-11}}$ **BNL E865** $\mathbf{\to < 10^{-11}}$	**31 TeV/c²**
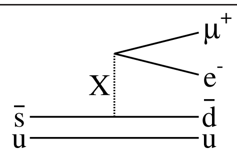	**Fermilab E799** $\mathbf{B(K^0_L \to \pi^0 \mu^\pm e^\mp) < 3.2 \times 10^{-10}}$	**37 TeV/c²**
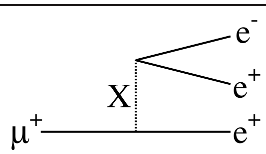	**PSI SINDRUM** $\mathbf{B(\mu \to eee) < 1.0 \times 10^{-12}}$	**86 TeV/c²**
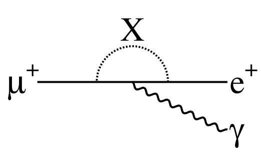	**MEGA** $\mathbf{B(\mu^+ \to e^+ \gamma) < 1.2 \times 10^{-11}}$ **Background limited** **PSI experiment** $\mathbf{\to 10^{-14}}$	**21 TeV/c²**
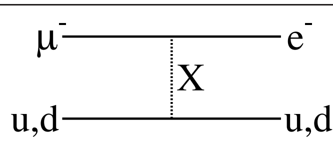	**PSI SINDRUM2** $\mathbf{R_{\mu e} = \frac{\Gamma(\mu^- A \to e^- A)}{\Gamma(\mu^- A \to \nu A')} < 6.1 \times 10^{-13}}$ **MECO at BNL** $\mathbf{\to 2 \times 10^{-17}}$	**365 TeV/c²**

- Hisano, hep-ph/0102315

$$\frac{R_{\mu e}}{Br(\mu \to e\gamma)} = 3 - 5 \times 10^{-3}$$

- Raidal, hep-ph/9710389
  Some models (SM with doubly charged scalar singlet coupled to the right-handed leptons) could have μ - e conversion enhanced by large logarithms:

$$\frac{R_{\mu e}}{Br(\mu \to e\gamma)} = 0.5 \ - \ 1$$

Values of Λ in TeV probed for different upper bounds of branching ratios:

R=	5×10^{-13}	3×10^{-14}
log-enhanced	101	158
non-enhanced	20	32
$\mu \to e\gamma$	70	141

Λ - is a mass scale responsible for new physics.

Predictions for $\mu - e$ conversion

- **Hisano et al., Phys. Lett. B391, 341 (1997)**

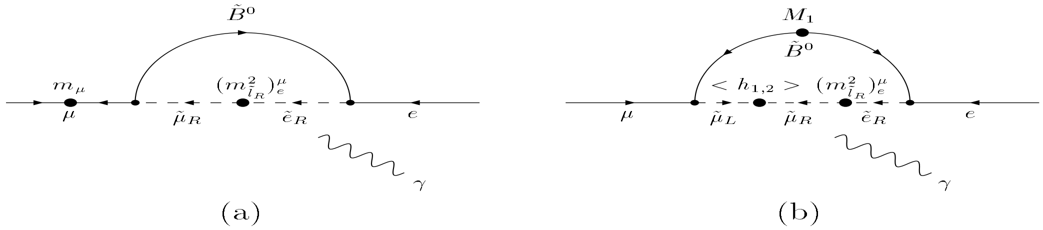

$\tilde{\mu}$ - smuon, ẽ - selectron, $\tilde{\mathrm{B}}^0$ - Bino, $\tilde{\mathrm{H}}^0$ - Higgsino

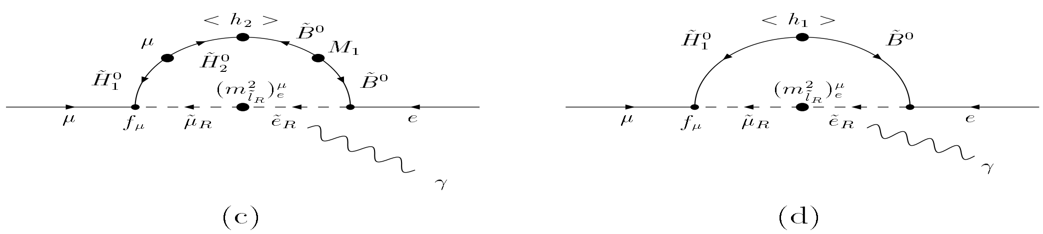

– **For example, minimal SUSY SU(5) has $\mathrm{R}_{\mu\mathrm{e}} \sim 10^{-14} - 10^{-17}$ over most of the parameter ranges.**

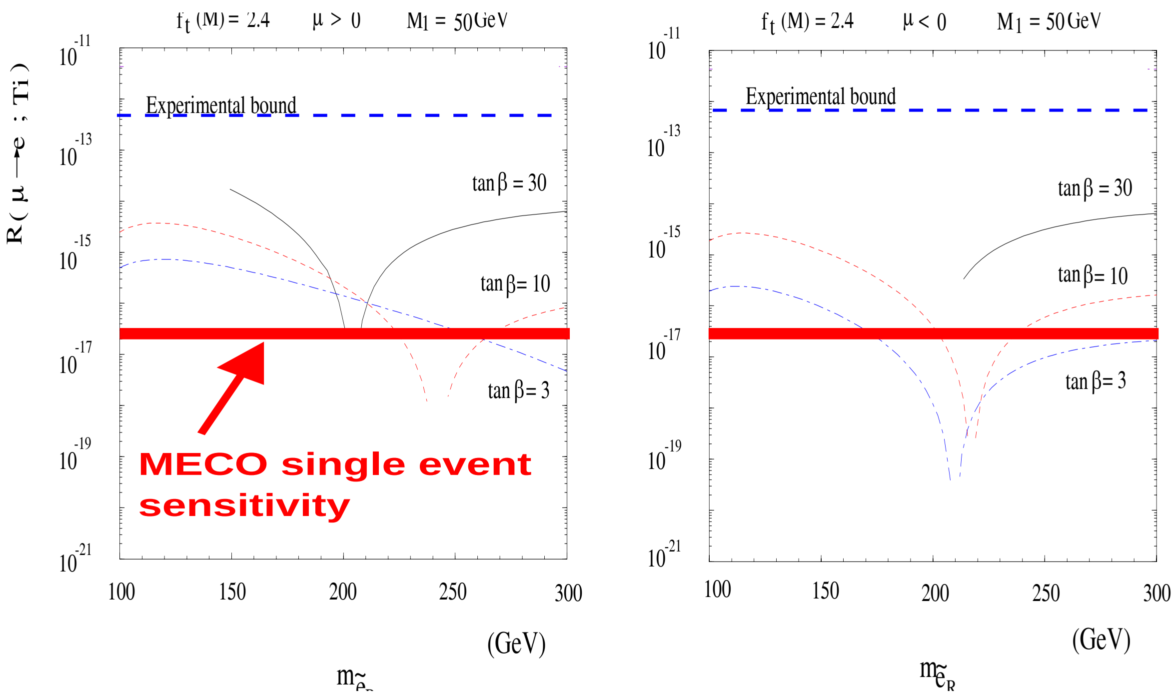

* - $\tan(\beta)$ is the ratio of the vacuum expectation values of the Higgs fields.

* - μ is Higgs fields' mixing parameter.

- **K.Tobe,hep-ph/0008085**
  - **If R-parity conservation is not postulated, additional terms in the MSSM superpotential are allowed:**

$$W_{RPV} = \frac{\lambda_{ijk}}{2} L_i L_j \bar{E}_k + \lambda'_{ijk} L_i Q_j \bar{D}_k,$$

where

- L_i **- left-handed doublet lepton,**
- $\bar{E}_i$ **- right-handed lepton,**
- Q_i **- left-handed doublet quark,**
- $\bar{D}_i$ **- right-handed down-type quark,**

Feynman diagrams with $\lambda_{131}\lambda_{231}$

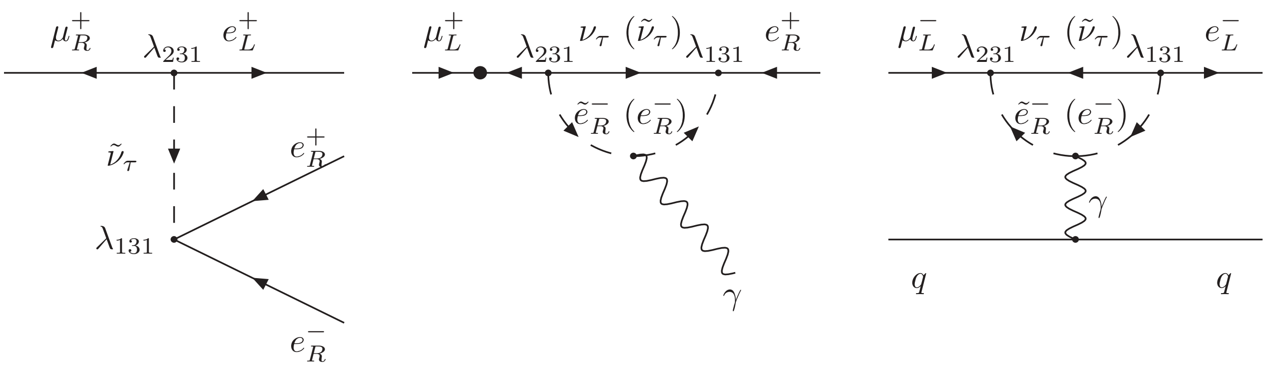

Feynman diagrams with $\lambda'_{121}\lambda'_{221}$

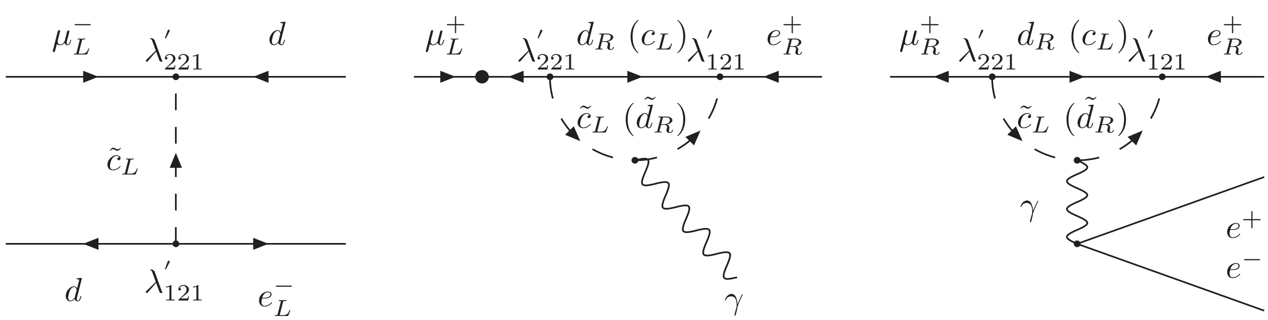

Table 1: Estimation of the ratio $\frac{R(\mu^- \to e^-)}{Br(\mu^+ \to e^+ e^- e^+)}$, assuming the contribution from only one dominant term.

$\lambda_{131}\lambda_{231}$	2×10^{-3}	$\lambda_{132}\lambda_{232}$	18	$\lambda'_{111}\lambda'_{211}$	3×10^{2}
$\lambda_{121}\lambda_{122}$	7×10^{-3}	$\lambda_{133}\lambda_{233}$	18	$\lambda'_{112}\lambda'_{212}$	8×10^{4}
$\lambda_{131}\lambda_{132}$	5×10^{-3}	$\lambda_{231}\lambda_{232}$	18	$\lambda'_{121}\lambda'_{221}$	2×10^{5}

- T.S.Kosmas,hep-ph/9904335,hep-ph/0002070
  - R-parity conservation diagrams
    - (a-c) – SM extentions
    - (d,e) – supersymmetric theories

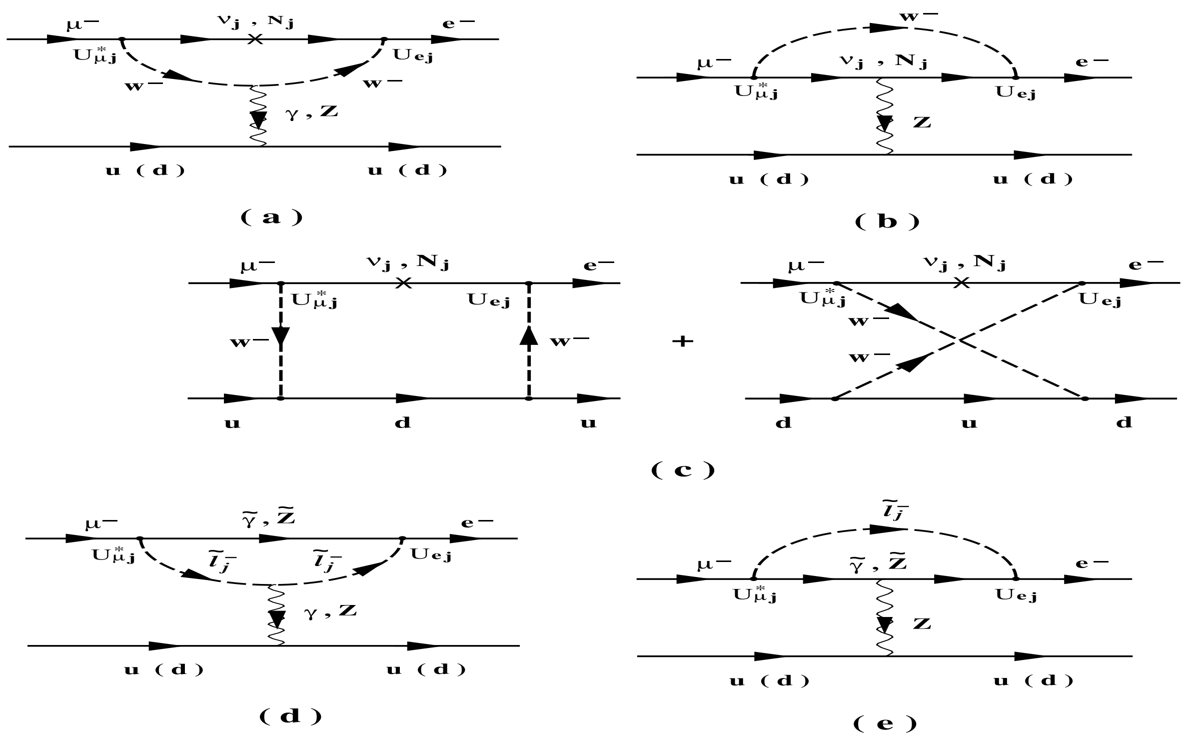

  - R-parity violating diagrams
    - The chargino-lepton mixing is schematically denoted by (X) on the lepton lines

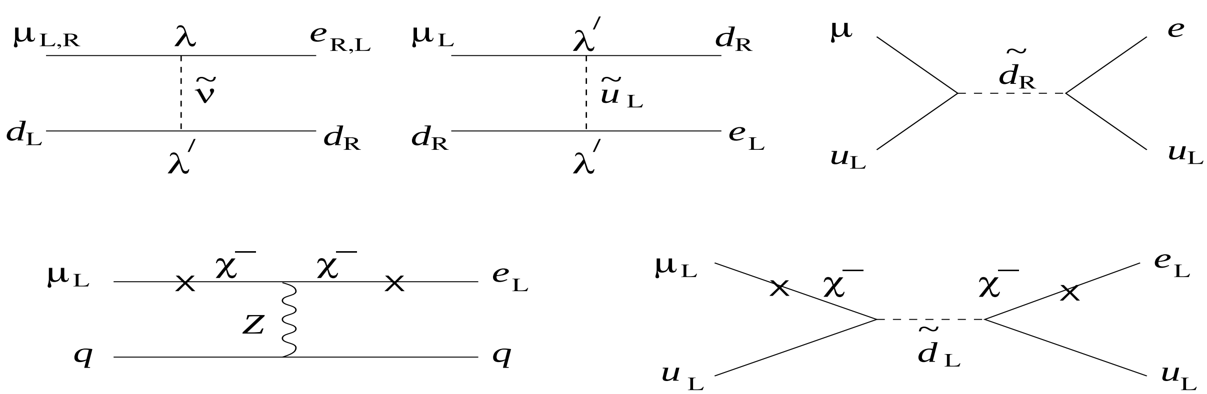

- **T.S.Kosmas,hep-ph/9904335,hep-ph/0002070**
  - $R_{\mu e} = \gamma(A, Z) \times \rho$
    - $\gamma(A, Z)$ **- nuclear physics part**
    - ρ **- elementary particle sector**

	^{27}**Al**	^{48}**Ti**	^{208}**Pb**	^{27}**Al**	^{48}**Ti**	^{208}**Pb**
experiment lim.				$\mathbf{1.7^{a} \times 10^{-17}}$	$\mathbf{7^{b} \times 10^{-13}}$	$\mathbf{4.9^{b} \times 10^{-10}}$
mechnism	γ			$\rho \times \mathbf{10^{19}}$	$\rho \times \mathbf{10^{14}}$	$\rho \times \mathbf{10^{13}}$
Photonic	4	9	17	46	82	32
W-boson exchange	34	25	49	6	3	11
SUSY sleptons	11	26	50	18	3	11
SUSY Z-exchange	28	111	236	7	0.7	2
$\not{R}_p$ SUSY	17	46	97	3	0.7	1.1

[a]MECO proposal

[b]SINDRUM II,Phys.Rev.Lett **76** 200 (1996); Phys.Atom.Nucl, G **1**, 1253 (1998)

- **Constraints on Youkawa couplings for R-parity violation models from** μ **- e conversion limits.**

Parameters	Previous limits	Present results ^{48}Ti$(\mu - e) \cdot B_{Ti}$	Expected results ^{27}Al$(\mu - e) \cdot B_{Al}$
$\lvert\lambda'_{211}\,\lambda'_{111}\rvert$	$4.4 \cdot 10^{-6}$	$6.2 \cdot 10^{-8}$	$4.0 \cdot 10^{-10}$
$\lvert\lambda'_{212}\,\lambda'_{112}\rvert$	$4.4 \cdot 10^{-6}$	$1.7 \cdot 10^{-8}$	$1.1 \cdot 10^{-10}$
$\lvert\lambda'_{213}\,\lambda'_{113}\rvert$	$4.4 \cdot 10^{-6}$	$1.7 \cdot 10^{-8}$	$1.1 \cdot 10^{-10}$
$\lvert\lambda'_{221}\,\lambda'_{111}\rvert$	$1.5 \cdot 10^{-5}$	$7.6 \cdot 10^{-8}$	$4.9 \cdot 10^{-10}$
$\lvert\lambda'_{222}\,\lambda'_{112}\rvert$	$1.5 \cdot 10^{-5}$	$7.6 \cdot 10^{-8}$	$4.9 \cdot 10^{-10}$
$\lvert\lambda'_{223}\,\lambda'_{113}\rvert$	$1.5 \cdot 10^{-5}$	$7.6 \cdot 10^{-8}$	$4.9 \cdot 10^{-10}$
$\lvert\lambda'_{231}\,\lambda'_{111}\rvert$	$[8.8 \cdot 10^{-5}]$	$8.3 \cdot 10^{-6}$	$5.3 \cdot 10^{-8}$
$\lvert\lambda'_{232}\,\lambda'_{112}\rvert$	$4.8 \cdot 10^{-4}$	$8.3 \cdot 10^{-6}$	$5.3 \cdot 10^{-8}$
$\lvert\lambda'_{233}\,\lambda'_{113}\rvert$	$4.8 \cdot 10^{-4}$	$8.3 \cdot 10^{-6}$	$5.3 \cdot 10^{-8}$
$\lvert\lambda'_{211}\,\lambda'_{121}\rvert$	$3.0 \cdot 10^{-5}$	$7.6 \cdot 10^{-8}$	$4.9 \cdot 10^{-10}$
$\lvert\lambda'_{212}\,\lambda'_{122}\rvert$	$3.0 \cdot 10^{-5}$	$7.6 \cdot 10^{-8}$	$4.9 \cdot 10^{-10}$
$\lvert\lambda'_{213}\,\lambda'_{123}\rvert$	$3.0 \cdot 10^{-5}$	$7.6 \cdot 10^{-8}$	$4.9 \cdot 10^{-10}$
$\lvert\lambda'_{221}\,\lambda'_{121}\rvert$	$8.0 \cdot 10^{-6}$	$1.4 \cdot 10^{-8}$	$9.0 \cdot 10^{-11}$
$\lvert\lambda'_{222}\,\lambda'_{122}\rvert$	$8.0 \cdot 10^{-6}$	$3.3 \cdot 10^{-7}$	$2.1 \cdot 10^{-9}$
$\lvert\lambda'_{223}\,\lambda'_{123}\rvert$	$8.0 \cdot 10^{-6}$	$3.3 \cdot 10^{-7}$	$2.1 \cdot 10^{-9}$
$\lvert\lambda'_{231}\,\lambda'_{121}\rvert$	$1.6 \cdot 10^{-4}$	$3.7 \cdot 10^{-5}$	$2.4 \cdot 10^{-7}$
$\lvert\lambda'_{232}\,\lambda'_{122}\rvert$	$1.6 \cdot 10^{-4}$	$3.7 \cdot 10^{-5}$	$2.4 \cdot 10^{-7}$
$\lvert\lambda'_{233}\,\lambda'_{123}\rvert$	$1.6 \cdot 10^{-4}$	$3.7 \cdot 10^{-5}$	$2.4 \cdot 10^{-7}$
$\lvert\lambda'_{211}\,\lambda'_{131}\rvert$	$[4.2 \cdot 10^{-4}]$	$8.3 \cdot 10^{-6}$	$5.3 \cdot 10^{-8}$
$\lvert\lambda'_{212}\,\lambda'_{132}\rvert$	$4.8 \cdot 10^{-4}$	$8.3 \cdot 10^{-6}$	$5.3 \cdot 10^{-8}$
$\lvert\lambda'_{213}\,\lambda'_{133}\rvert$	$[1.2 \cdot 10^{-5}]$	$8.3 \cdot 10^{-6}$	$5.3 \cdot 10^{-8}$
$\lvert\lambda'_{221}\,\lambda'_{131}\rvert$	$1.6 \cdot 10^{-4}$	$3.7 \cdot 10^{-5}$	$2.4 \cdot 10^{-7}$
$\lvert\lambda'_{222}\,\lambda'_{132}\rvert$	$1.6 \cdot 10^{-4}$	$3.7 \cdot 10^{-5}$	$2.4 \cdot 10^{-7}$
$\lvert\lambda'_{223}\,\lambda'_{133}\rvert$	$[1.2 \cdot 10^{-5}]$	$3.7 \cdot 10^{-5}$	$2.4 \cdot 10^{-7}$
$\lvert\lambda'_{231}\,\lambda'_{131}\rvert$	$3.5 \cdot 10^{-5}$	$1.3 \cdot 10^{-8}$	$8.3 \cdot 10^{-11}$
$\lvert\lambda'_{232}\,\lambda'_{132}\rvert$	$3.5 \cdot 10^{-5}$	$4.0 \cdot 10^{-3}$	$2.6 \cdot 10^{-5}$
$\lvert\lambda'_{233}\,\lambda'_{133}\rvert$	$3.5 \cdot 10^{-5}$	$4.0 \cdot 10^{-3}$	$2.6 \cdot 10^{-5}$

- **B.Murakami,hep-ph/0111065**
  String and Technicolor models

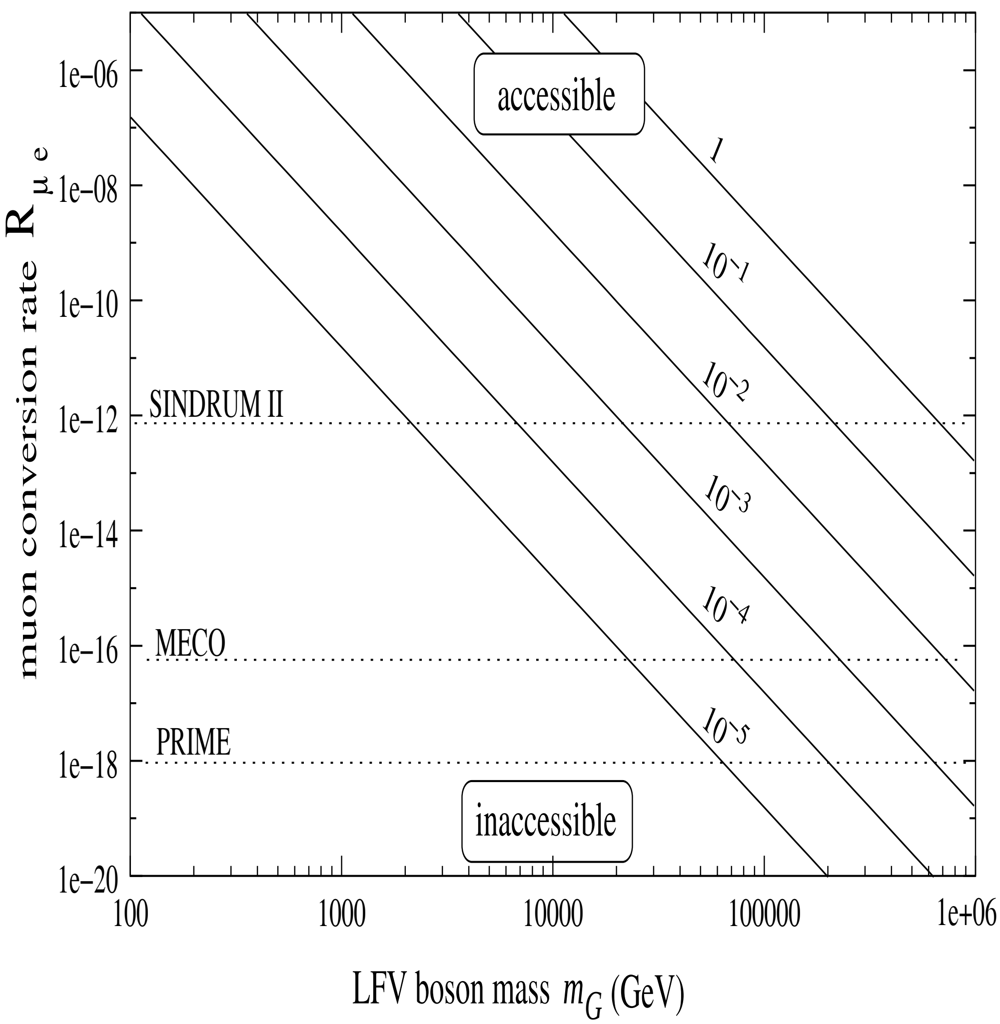

- **J.Ellis, hep-ph/0103256**

m_0 vs $m_{1/2}$

m_0 - symmetry-breaking masses for sfermions; $m_{1/2}$ – for gauginos

– **Allowed area:**

  * – preferred from cosmology
  * – g-2 experiment

(Should be changed after recent correction - hep-ph/0112102 !)

– **Excluded area:**

  * – astrophysical requirement that cold dark matter is electrically neutral
  * – from $b \to s\gamma$ constraint

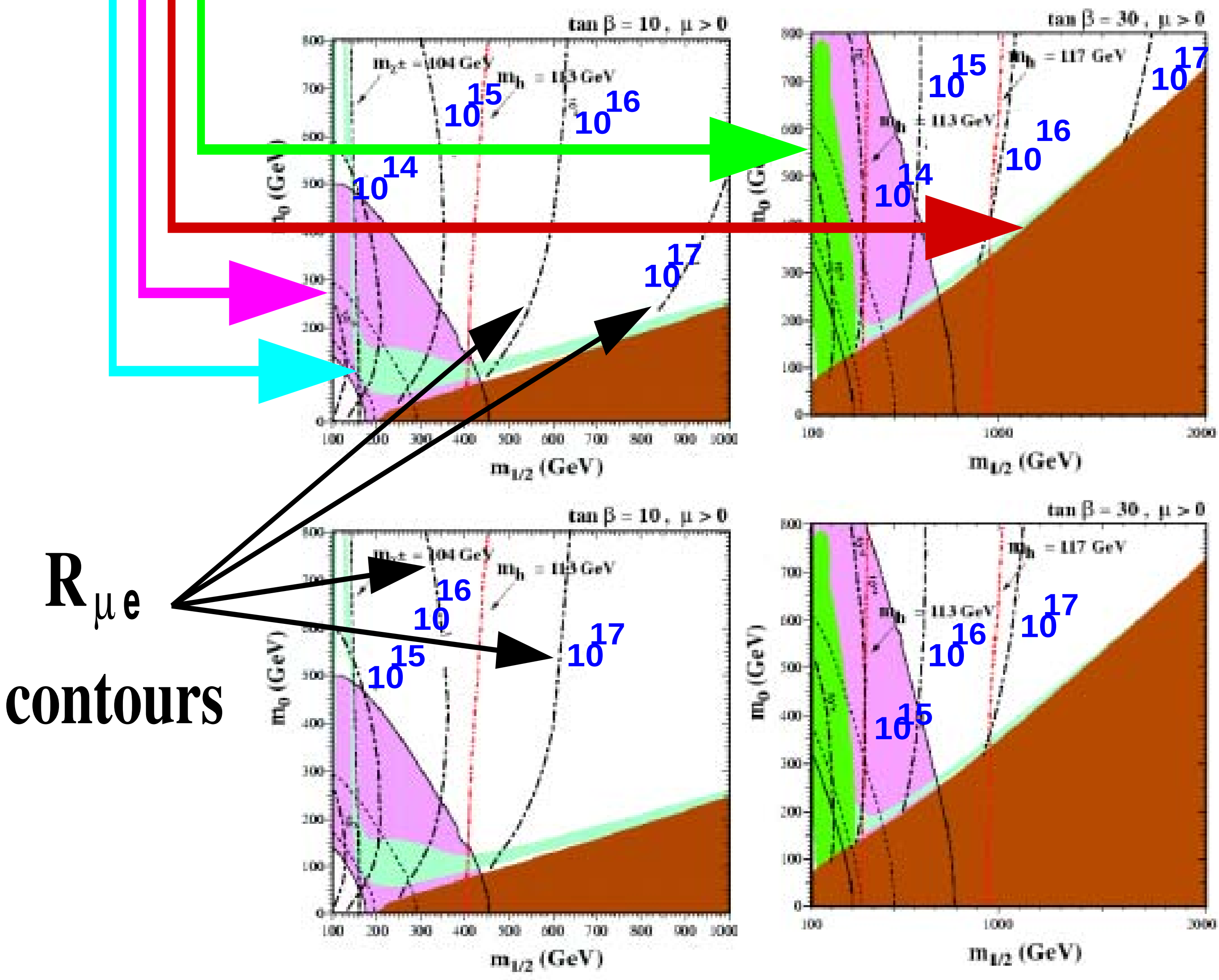

- **W. Marciano, not published**

Parameter value for $R_{\mu e} = 10^{-16}$

– **Super-symmetry:**

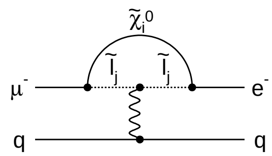

predictions at 10^{-15} level

– **Heavy neutrinos:**

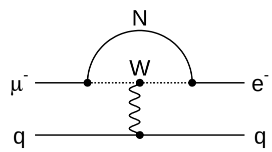

$|U^*_{\mu N} U_{eN}|^2 = 8 \times 10^{-13}$

– **Leptoquarks:**

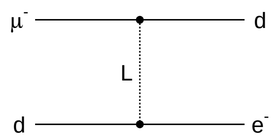

$M_{LQ} = 3000\ (\lambda_{\mu d}\lambda_{ed})^{1/2}\ \mathrm{TeV/c^2}$

– **Compositeness:**

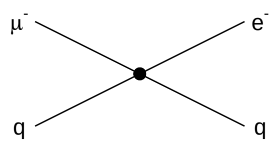

$\Lambda_C = 3000$ TeV

– **Neutral Higgs:**

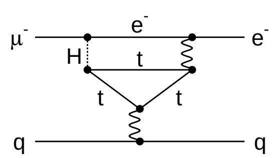

$g_{H_{\mu e}} = 10^{-4} \times g_{H_{\mu\mu}}$

– **Heavy Z', anomalous Z coupling:**

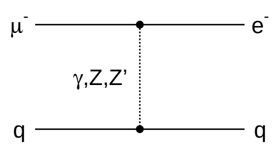

$M_{Z'} = 3000\ \mathrm{TeV/c^2}$
$B(Z \to \mu e) < 10^{-17}$

Figure 1: Feynman diagrams for the process $\mu^- N \to e^- N$ in different scenarios for non-Standard Model physics, with parameter limits in specific models for a value of $R_{\mu e} = 10^{-16}$. This figure is after the work of W. Marciano.

Coherent μ^- to e^- Conversion: $\mu^- N \to e^- N$

– μ^- stop in materials by slowing to thermal-like velocities through inelastic atomic collisions, then eventually falling into an orbit about a nucleus.

– Bohr (point charge nucleus):

$$E_n = -m_\mu \frac{(Z\alpha)^2}{2n^2} \quad \text{and} \quad r_n = \frac{n^2}{Z\alpha m_\mu}.$$

– The excited states cascade to the 1S ground state producing X rays and Auger electrons.

– For our choice of stopping target: Aluminum ($Z = 13,\ A = 27$)

  * $\tau_{\text{free}} = \mathbf{2.2}\,\mu$s
  * Mean bound muon lifetime is $\tau(\text{Al}) = 880\,$ns,

– Two things happen to the μ^- nearly all the time:

		Aluminum
Nuclear capture	$\mu^-\mathbf{N(Z,A)} \to \nu_\mu \mathbf{N(Z-1,A)}$	$\sim 60\%$
Decay in orbit	$\mu^-\mathbf{N(Z,A)} \to \nu_\mu \mathbf{e}^- \overline{\nu}_e \mathbf{N(Z,A)}$	$\sim 40\%$

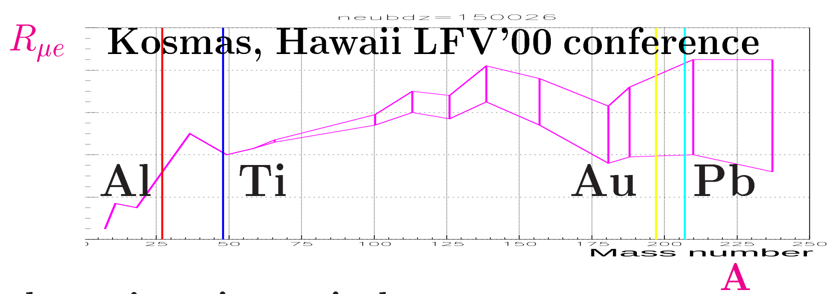

Why Aluminum ?

$\ominus$ $\frac{R^{Al}_{\mu e}}{R^{Ti}_{\mu e}} \simeq 0.6;$

$\oplus$ $\tau^{Al} > \tau^{Ti} = 329$ ns $\Rightarrow$ detection time window 700-1350 ns well beyond the arrival time of prompt background particles at the stopping target

$\oplus$ very pure Al with known end-point of DIO energy spectrum $\hookleftarrow$ low Z impurity in a high Z target can produce an electron with energy beyond the nominal end-point

– μ- e conversion in muonic atom:

		Aluminum
Coherent:	$\mu^-\mathbf{N(Z,A)} \to \mathbf{e}^-\mathbf{N(Z,A)}$	$\sim 80\%$
Incoherent:	$\mu^-\mathbf{N(Z,A)} \to \mathbf{e}^-\mathbf{N}^*\mathbf{(Z,A)}$	$\sim 20\%$

μ - e conversion signature

– Only e^- in coherent channel exp. distinguishable.
  Coherence ⇒ enhancement in the transition rate:
  * Extra factor of Z in the rate.
  * Elastic form factor large at conversion energy.

– Look for distinctive two-body final state:

$$\mu^- + \mathrm{N}(\mathbf{Z},\mathbf{A}) \to \mathbf{e}^- + \mathrm{N}(\mathbf{Z},\mathbf{A})\,.$$

  * Initial & final internal nuclear states same.
  * Signature : Mono-energetic electron

$$\mathbf{E_e} = \mathbf{E}_\mu - \frac{\mathbf{E}_\mu^2}{2\mathbf{M_A}} \quad \text{and} \quad \mathbf{E}_\mu = \mathbf{m}_\mu + \mathbf{E}(\mathbf{1s}),\ \ \mathbf{M_A} = \mathbf{1GeV/c^2},$$

  in time window delayed with respect to beam pulse.
  * $\mathbf{E_e}(\mathrm{Al}) = \mathbf{105\,MeV}$.

– What makes this process experimentally attractive is:
  * The signature is simple
    (a single mono-energetic electron).
  * Detect only one particle: there is
    no accidental coincidence background
    at high rates, as in $\mu \to \mathrm{e}\gamma$.
  * Other sources of electrons
    at the conversion energy are
    heavily suppressed.

Current and future $\mu^- N \to e^- N$ experiments

TRIUMF

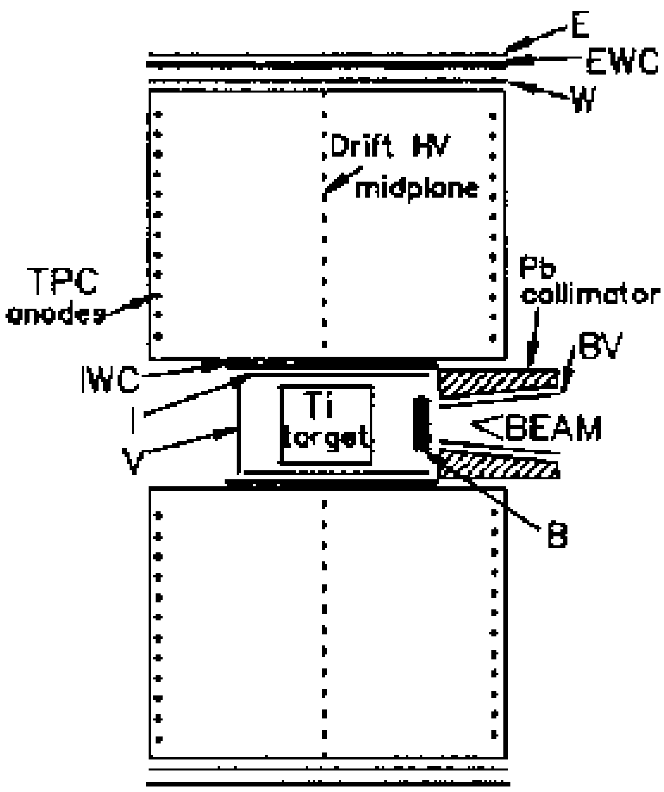

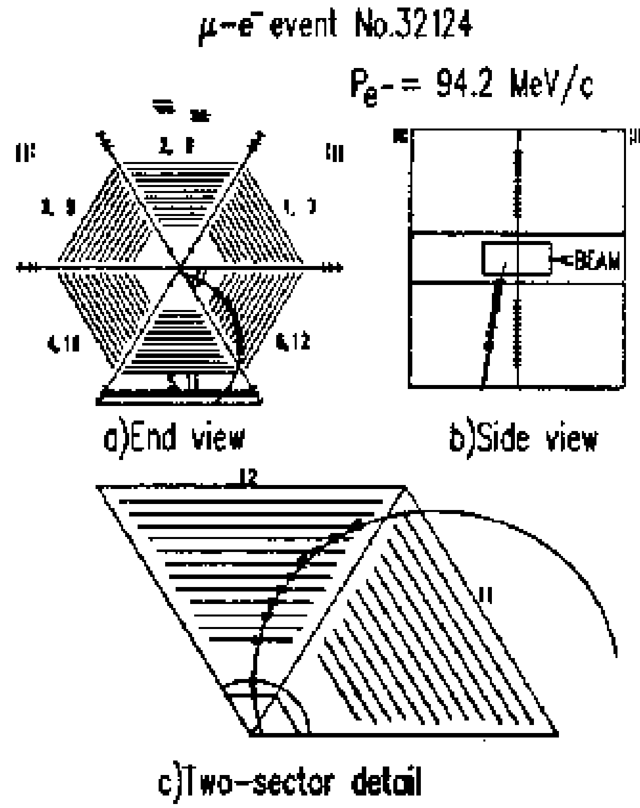

SINDRUM2

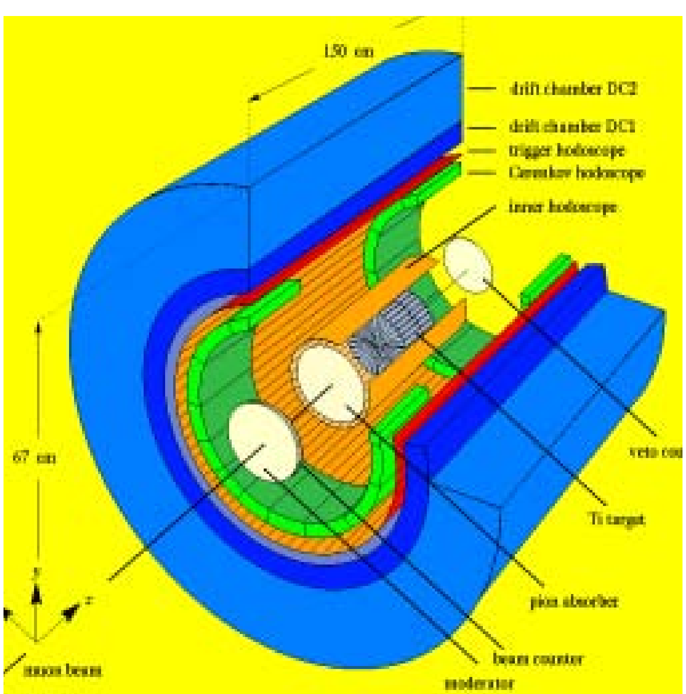

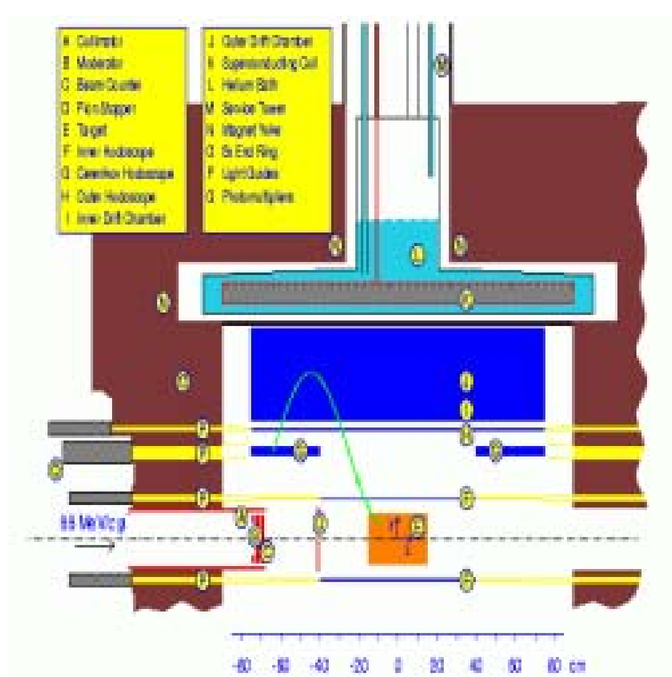

MECO

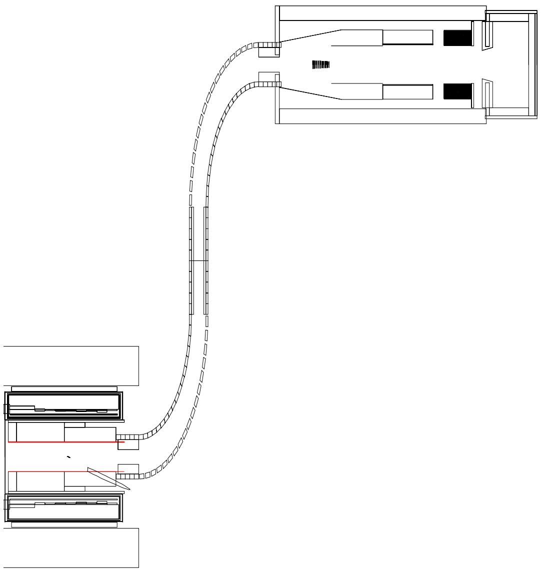

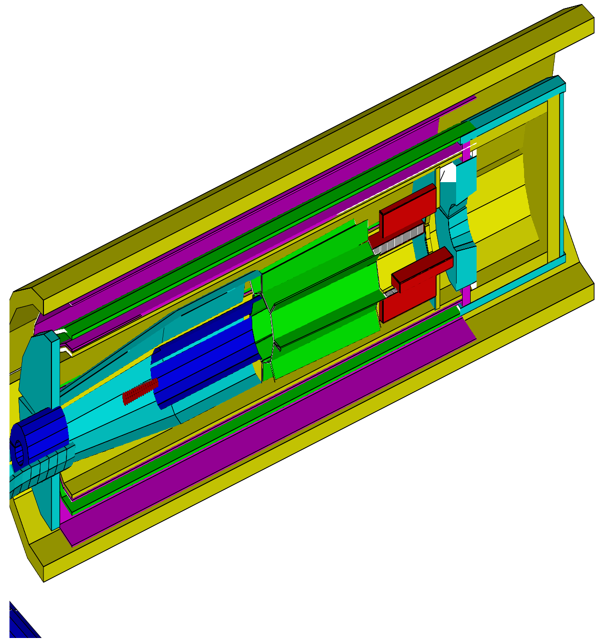

PRISM

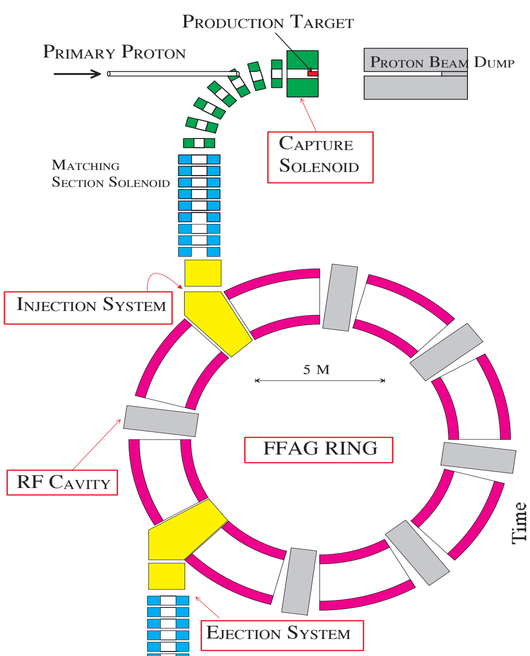
PRODUCTION TARGET
PRIMARY PROTON
PROTON BEAM DUMP
CAPTURE SOLENOID
MATCHING SECTION SOLENOID
INJECTION SYSTEM
5 M
FFAG RING
RF CAVITY
EJECTION SYSTEM

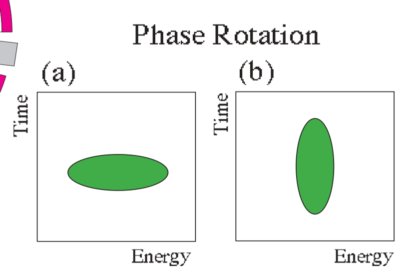
Phase Rotation
(a)
(b)
Time
Energy
Time
Energy

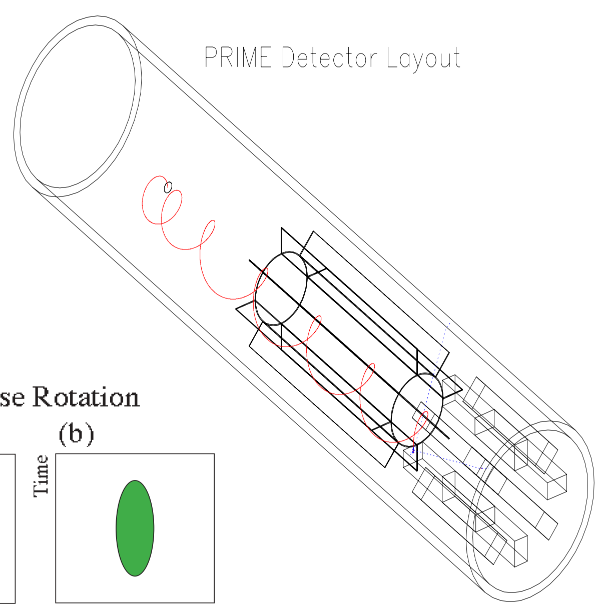
PRIME Detector Layout

Main features of two most recent and proposed experiments

	TRIUMF	SINDRUM2	MECO	PRISM
Tr. detector	TPC	Drift Chamber	Straw tubes	Straw tubes
Mag.field ,T	0.9	1.2	1.0	
Target	Ti 20 cm ($\rho = 0.1\frac{g}{cm^3}$)	Ti $16 \times 125\mu$	Al $17 \times 200\mu$	Ti $20 \times 50\mu$
μ^-_{in},[Hz]	1.3×10^6	12×10^6	2.5×10^{11}	1×10^{12}
μ^-_{stop}/μ^-_{in}, %	77	27	48	80
π/μ stops	10^{-4}	10^{-7}	10^{-11}	-
Reject Prompts	beam counters	beam counters	pulsed beam	pulsed beam & EAring
FWHM,[MeV]	4.5	2.3	0.9	0.35
Cosmic bckg.	∼0.15 / MeV	-	-	
Accpt., %	5.6	5.9	8.4	
Limit	4.6×10^{-12}	6.1×10^{-13}	5×10^{-17}	1×10^{-18}

Essential improvements in the MECO experiment:

- Significantly higher muon beam intensity.
- Usage of pulsed beam for time separation from prompt background.
- By means of graded magnetic field in the stopping target region conversion electrons are projected forward in helical trajectories, which allows to displace detectors several meters downstream and thus separate zone with high background rate from the products of the muon capture in the target and detector region.

† PRISM has some new good ideas, but the project in not developed in details.

Beam requirements:

- low energy,
- high intensity,
- beam time structure with short ($\ll \tau_\mu$) pulses separated by $\sim \tau_\mu$.
- extinction $10^{-9} - 10^{-10}$

BNL accelerator parameters:

- Revolution time 2.7 μs (6 RF buckets)
- Fill 2 RF buckets 1.35 μs apart
- Machine transition at $\mathbf{p} \approx \mathbf{8GeV}$ GeV/c
- $\mathbf{4 \times 10^{13}}$ protons/sec
- Cycle time 1.0 s 50% duty factor
- Resonantly extract bunched beam

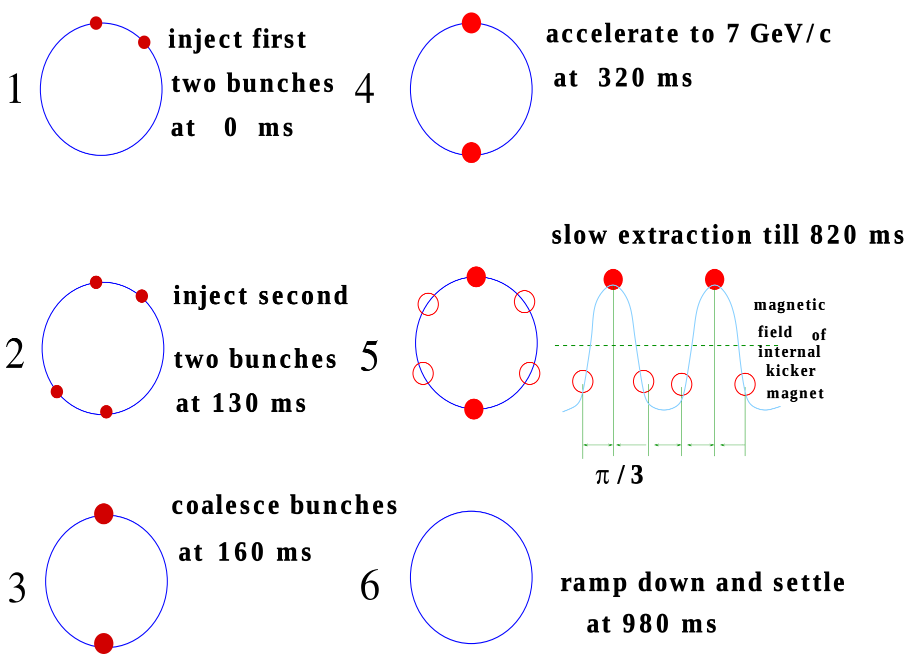

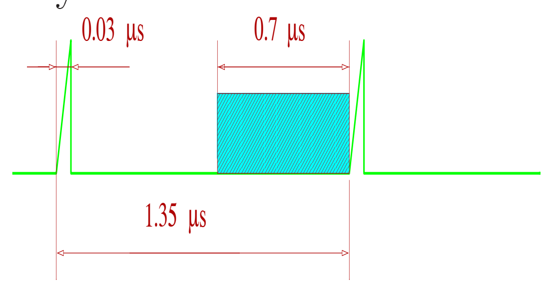

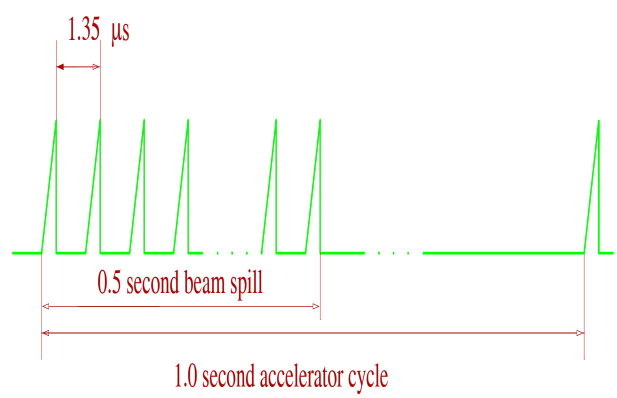

Extinction

- Measurements in E871 experiment and measurements of in E787 experiment confirmed that extinction between the buckets and in unfilled buckets of AGS is of order $\sim 1.0 \times 10^{-7}$.
- Internal kicker magnet and external RF modulated magnet to improve extinction.

Target: W, 16cm long,ϕ0.8cm, 42cm^2, 156g, 4.7kW

Radiative cooled: $P = \epsilon \sigma A T^4$

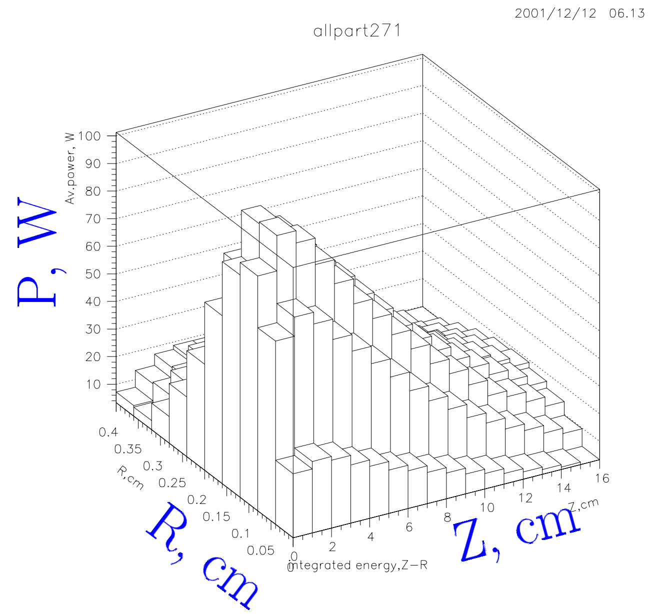

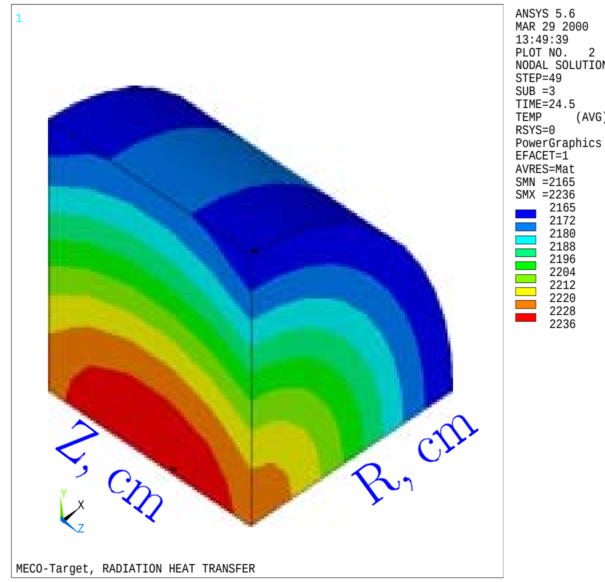

Temp. K	Yield strength MPa
300	1519
500	150
1000	110
1500	75
2000	40
2500	20
3000	NA

Slice Thickness(mm)	8	4	4	2	1
Slice Spacing (mm)	8	8	8	8	8
Emissivity	.9	.4	.9	.9	.9
Max T on spill (K)	2396	2705	2236	2032	1803
Axial Stress (MPa)	85.8	18.1	18.2	2.5	1.0
Hoop stress (MPa)	-95.1	-20.5	-20.0	-2.5	-0.7
Radial stress (MPa)	-83.5	-74.5	-72.2	-44.9	-29.9
Von Mises (MPa)	-87.1	-74.4	-72.1	-45.0	-30.1

- Stresses are larger than Tungsten yield strength at this temperature
- Subdivision on thin disks could be a solution. **More study is needed !**

Water cooled:

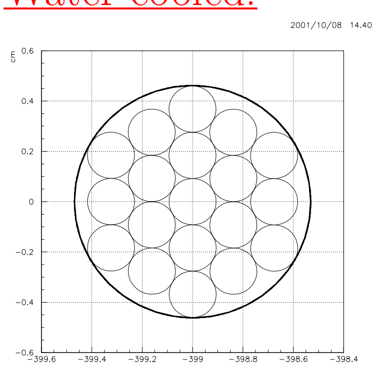

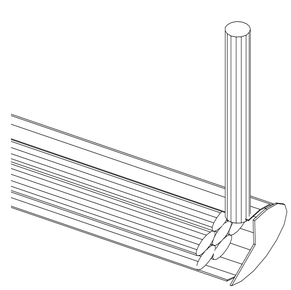

- 19-W rods, 1.0 mm dia.
- turbulent flow between rods
- $\sim$ 5–7 atm, $<$ 2 gal/min
- non-boiling condition

- Stresses are smaller, because of small rod diameter
- Tungsten yield strength at room temperature is much larger than that at 2500K

Production solenoid system physics requirements

- Requirements:
  - Field and bore appropriate to capture most low energy pions produced in the target and to direct them to the transport solenoid.
  - Able to operate in the radiation environment from 50kW proton beam interacting in the target.
- Implementation:
  - 5 T field at upstream end, axially graded to 2.5 T at the beginning of the transport solenoid.
  - 1.5 m diameter clear bore allowing 45-55 cm thick shield, 40-60 cm diameter clear area.

Production solenoid in GEANT simulation.

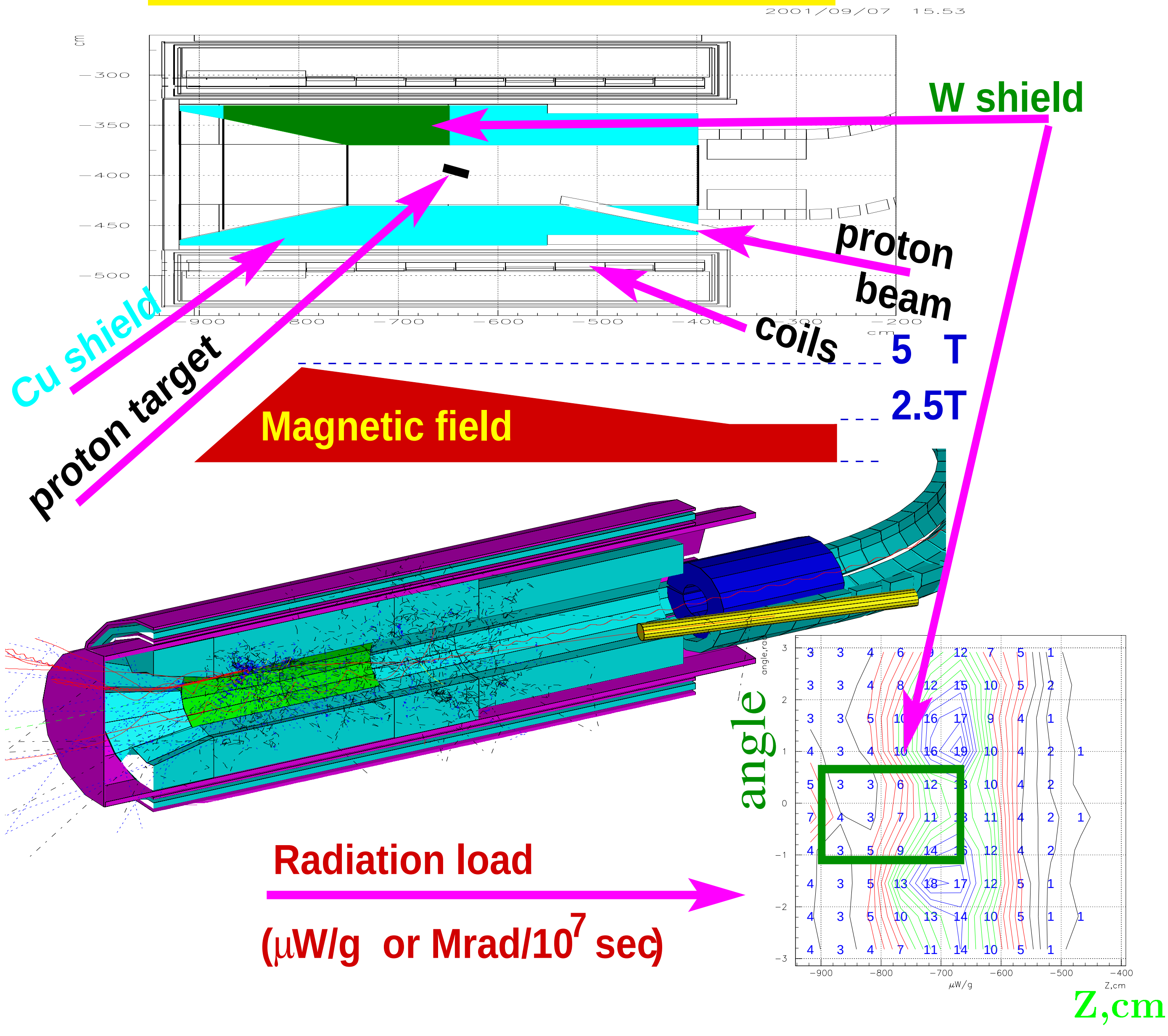

MECO Superconducting Solenoids

- 1999 - National High Magnetic Field Laboratory (NHMFL) at Florida State Uninersity - pre-conseptual design of MECO magnetsystem.
  - major design issues
  - preliminary cost and schedule estimates
- 2001 - Massachusetts Institute of Technology (MIT) - Conseptual Design Study Contract
  - magnetic design
  - cable, coil design
  - forces and stresses in the magnetic system
  - cooling mechanism, cryogenic system
  - vacuum system

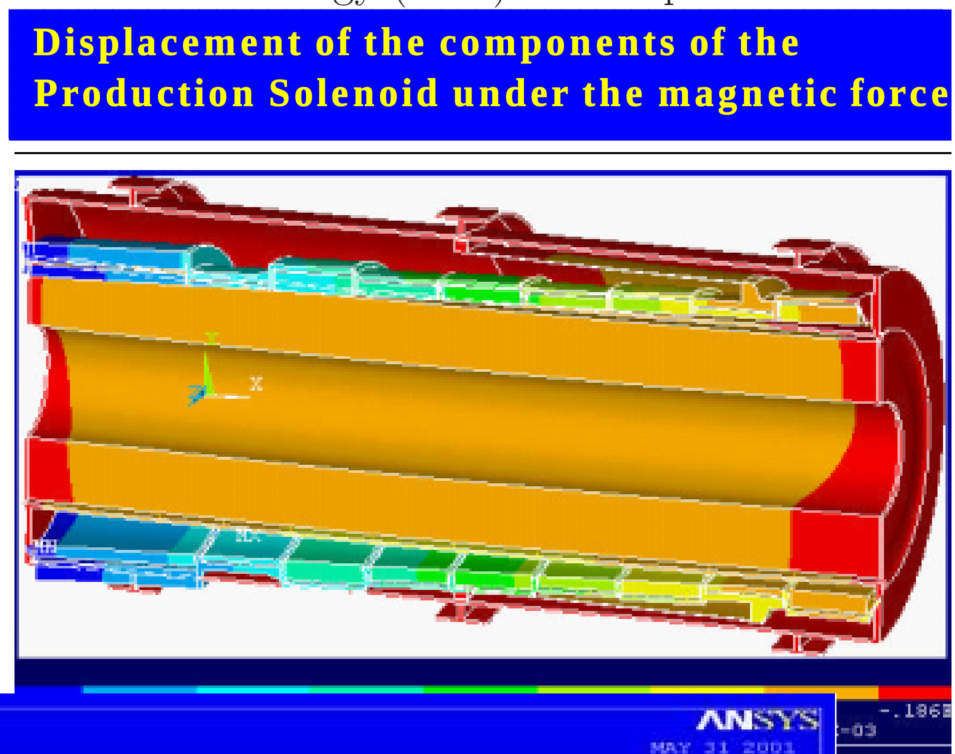

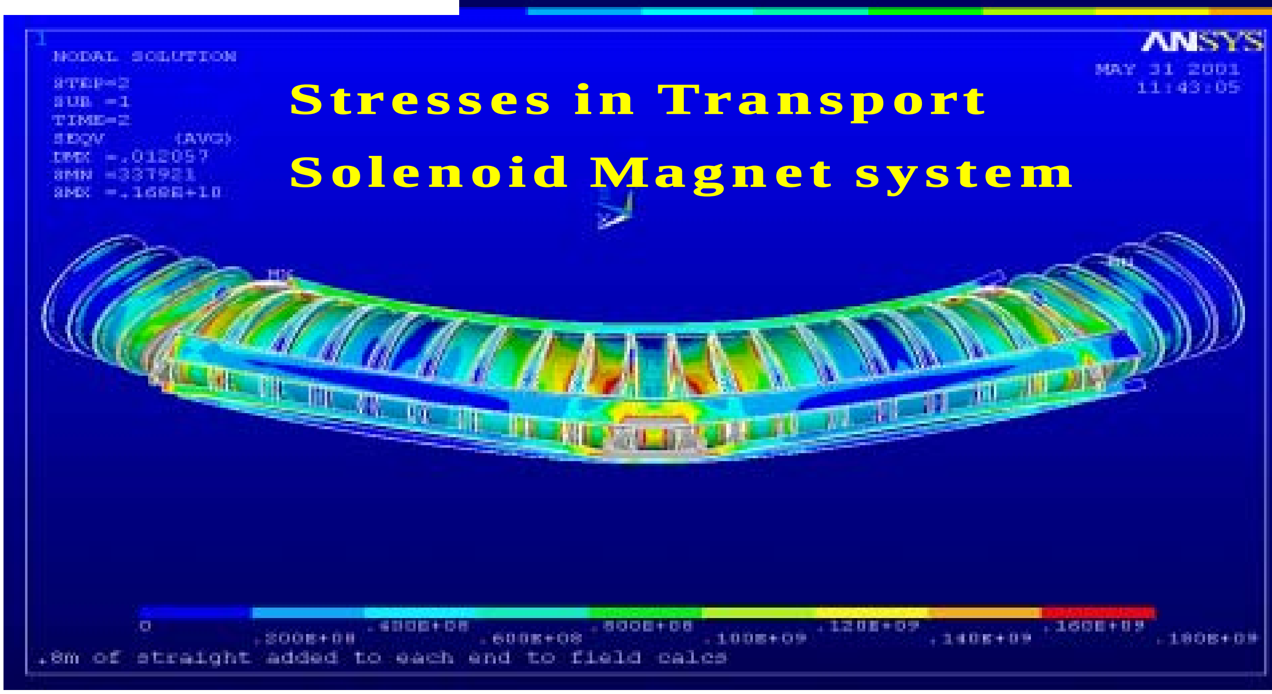

Transport solenoid:

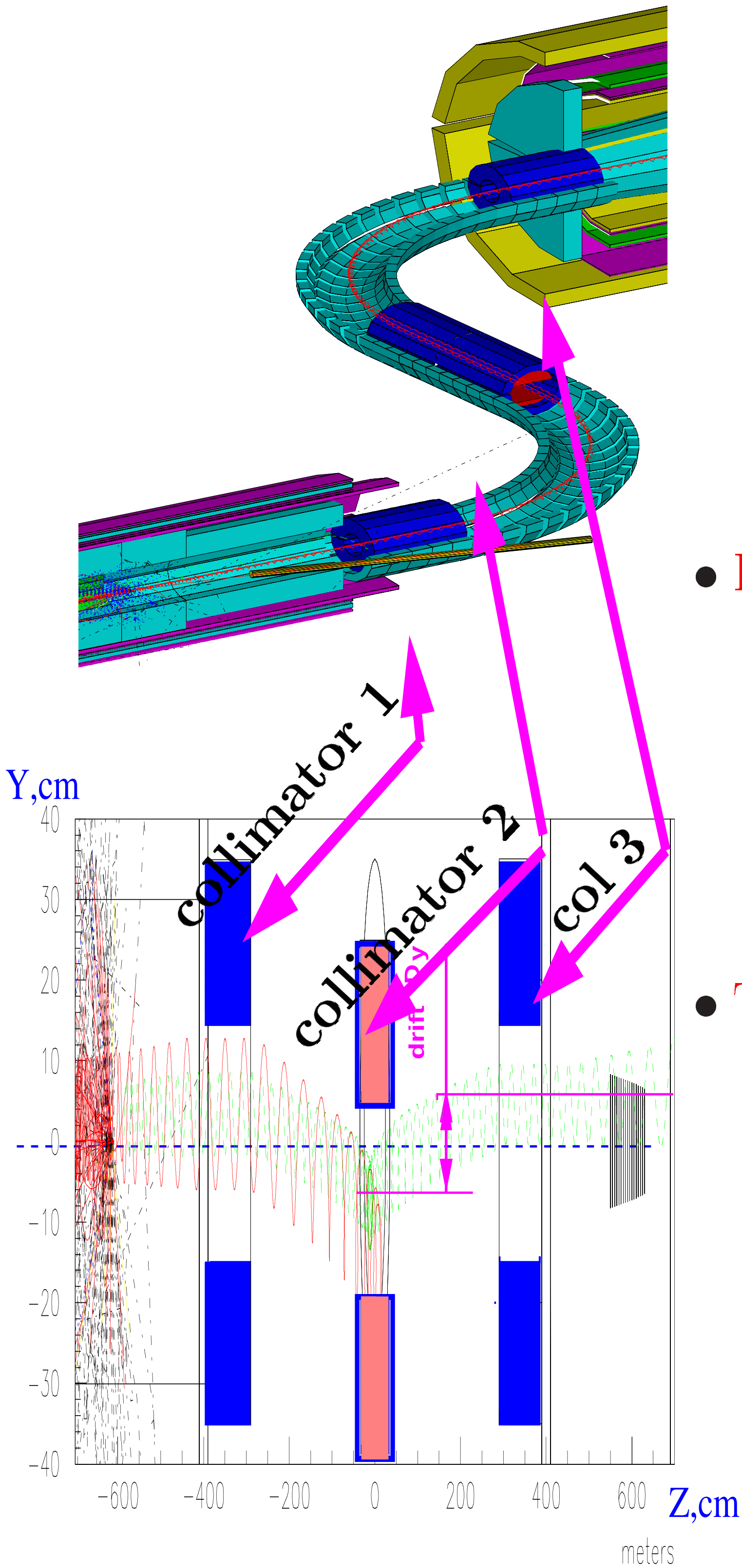

- Requirements:
  - Transport low energy negative muons from the Production Solenoid to the Detector Solenoid
  - Minimize transport of positive and neutral (neutrons and photons) particles and high energy particles
- Implementation:
  - Curved magnet system which transport low energy negative particles and drive all other charged particles into the collimators.
- Transverse particle drift
  - $D_y = \frac{A}{0.3B} \times \frac{p_a^2 + 0.5 p_t^2}{p_a}$
    where
    * Magnetic field B=2 T
    * A=$\pi/2$ – bend angle of solenoid
    * p_t, p_a – transverse and longitudinal momentum components

Detector solenoid:

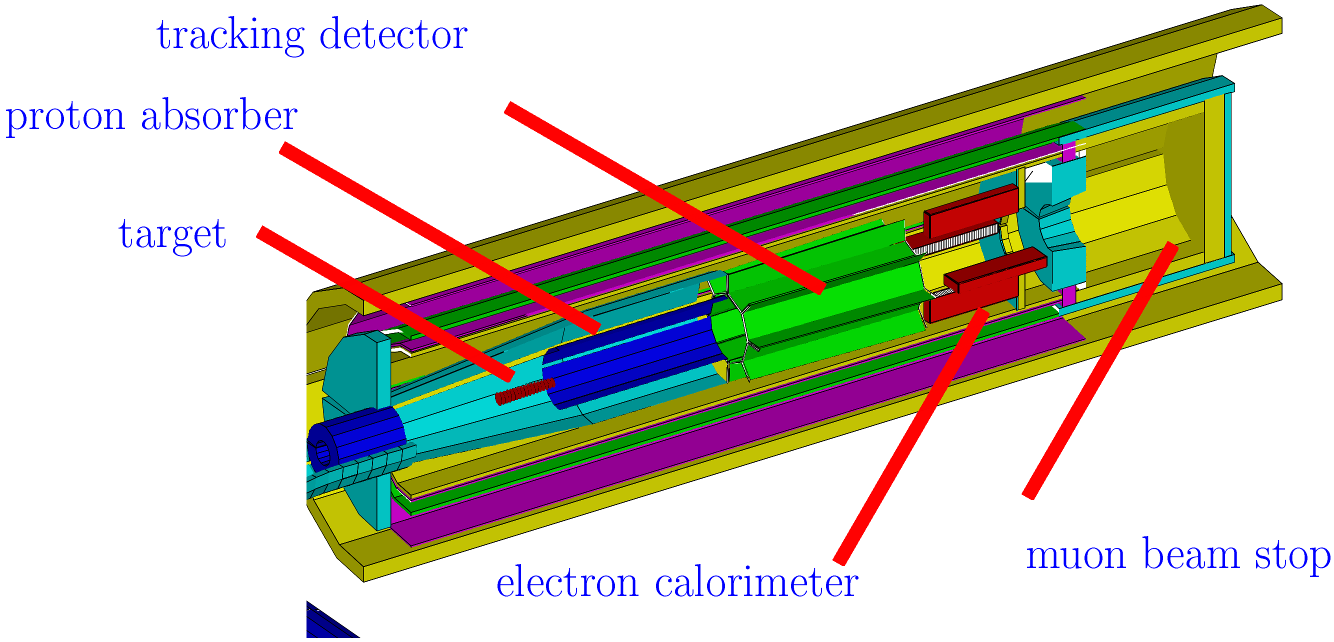

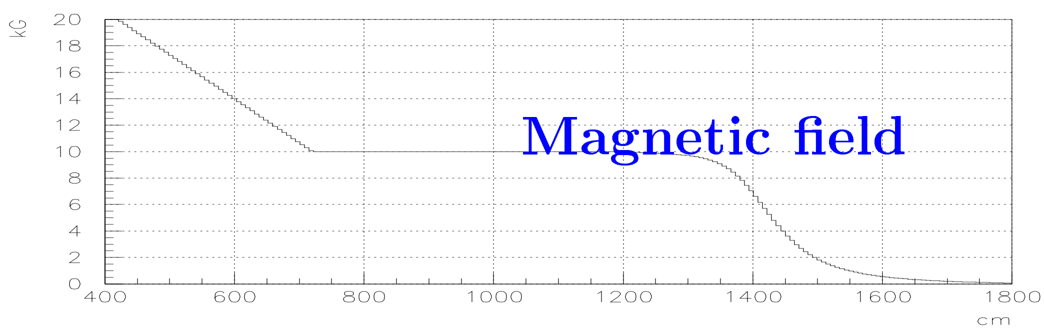

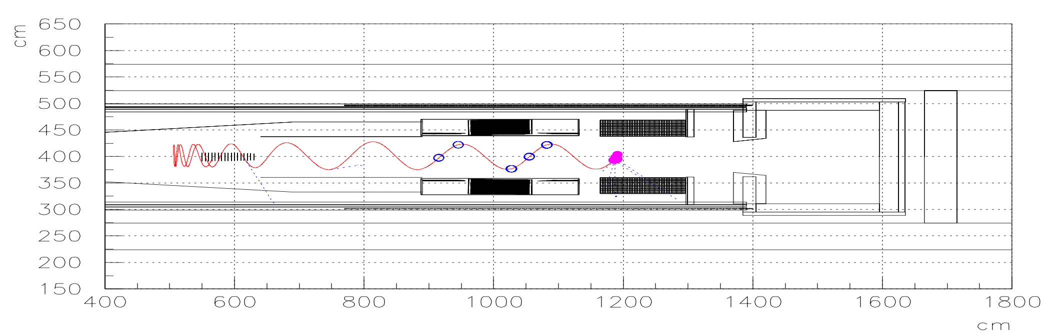

Only electrons with energy above 55 MeV can hit tracking detector and electron calorimeter !

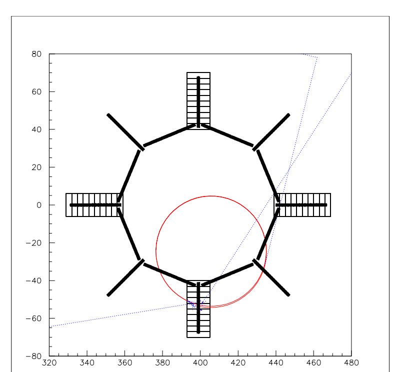

MECO Detector Resolution Studies

- Excellent resolution to eliminate μ^- DIO background
- Full GEANT simulation of detector response
- Electron energy fitted by maximum likelihood method
  – FWHM $\sim$ 900 keV, no high energy tail
- Selection criteria chosen to reduce background

Selection criterion	Efficiency
At least 6 clusters in tracking detector	0.44
Detected energy above $\sim$103.6 MeV	0.62
Required pitch angle at the detector	0.88
Requirements on fitting quality	0.83
Position match in electron calorimeter	0.97
Overall acceptance	0.19

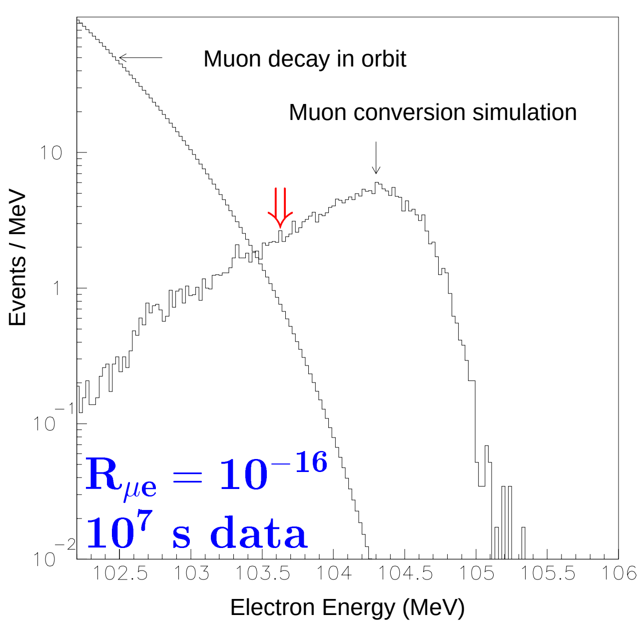

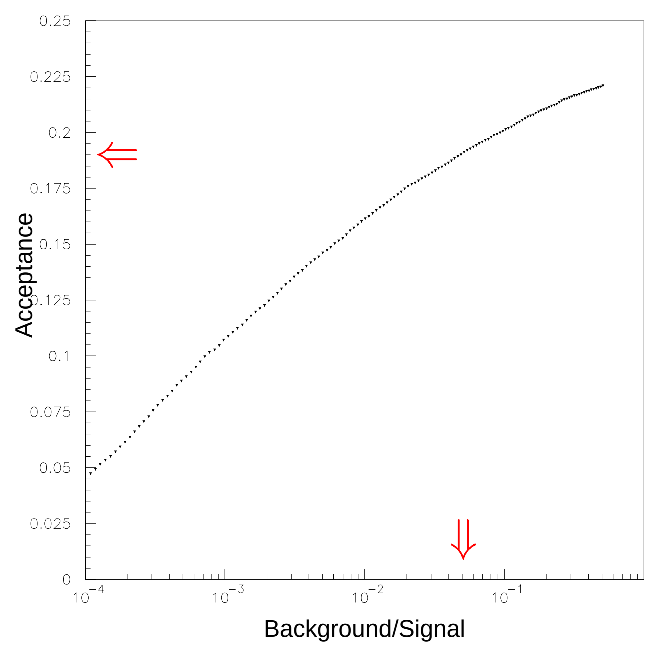

Improved background rejection available with small loss in sensitivity

Expected MECO Sensitivity and Backgrounds

Sensitivity per year of running:

Running time (s)	10^7
Proton flux (Hz)	4×10^{13}
μ/p entering solenoid	0.0043
Stopping probability	0.58
μ capture probability	0.60
Fraction of μ capture in time window	0.49
Electron trigger efficiency	0.90
Fitting and selection criteria	0.19
Detected events for $R_{\mu e} = 10^{-16}$	5.0

Expected background:

Source	Events	Comment
μ^- decay in orbit	0.25	S/N = 20 for $R_{\mu e} = 10^{-16}$
Tracking errors	< 0.006	
Radiative μ^- capture	< 0.005	
Beam electrons	< 0.04	
μ^- decay in flight	< 0.03	no scatter in target
μ^- decay in flight	0.04	scatter in target
π^- decay in flight	< 0.001	
Radiative π^- capture	0.07	out of time protons
Radiative π^- capture	0.001	late arriving π^-
Anti-proton induced	0.007	
Cosmic ray induced	0.004	10^{-4} CR veto ineff.
Total background	0.45	Assumes 10^{-9} extinction

History of MECO Project Status

September	1996	MECO Letter of Intent considered by BNL PAC. **Collaboration encouraged to submit full proposal.**
October	1997	**MECO proposal approved by BNL.**
February	1998	**Gilman HEPAP subpanel recommends DOE support for 2 experiments using unique AGS facilities.**
December	1998	**Initial contact with NSF regarding construction funding.**
September	1999	RSVP proposal for construction of MECO and KOPIO experiments submitted to NSF.
December	1999	NSF panel reviews scientific and technical merit of MECO and other experiments – **recommends funding MECO.**
August	2000	RSVP Major Research Equipment (MRE) proposal presented by NSF to the National Science Board.
October	2000	**NSB approves resolution requesting funding for RSVP in this or a future fiscal year.**
March	2001	**$1.5M R&D budget approved for MECO.**
June	2001	NSF Project Review.
September	2001	MIT Interim Design Review.
September	2001	Applied NSF R&D grant: additional design and development.
December	2001	MIT Conceptual Design Report for magnet system.
October	2003	?? Begin construction at BNL ??

Conclusion

We are ready for the experiment !

- **40 Tp pulsed 8 GeV proton beam**
- **High Z production target in graded solenoidal field**
- **Muon transport in curved solenoid**